

Synthesis, Spectral Characterization, and Antimicrobial Properties of Mixed-Ligand and Their Metal (II) Complexes

Prabhakar Chavan ^{1,*}, M. M. Nagabhushana ², P. Parameshwara Naik ¹, J B Varunakumara ³, Prashant C. Hanamshetty ⁴, A. Thippeswamy ⁵

¹ Department of Studies and Research in Chemistry, Sahyadri Science College, Shivamogga-577203, Karnataka, India; prabhakarc@kussc.ac.in (P.C.); parashchem@gmail.com (P.P.N.);

² Department of Chemistry, Govt. Engineering College, Raichur-585135, Karnataka, India; bushichem@gmail.com;

³ Department of Biochemistry, Sahyadri Science College, Shivamogga-577203, Karnataka, India; varuna24july@gmail.com;

⁴ Department of Chemistry, Guru Nanak First Grade College, Bidar, Karnataka, India; prashant.hanamshetty@gmail.com;

⁵ Government Arts and Science College (autonomous), Karwar, Karnataka, India; naikthippu@gmail.com;

* Correspondence: prabhakarchavan7@gmail.com;

Received: 2.04.2025; Accepted: 17.07.2025; Published: 25.11.2025

Abstract: The present study reports the synthesis, structural characterization, and biological evaluation of Cu(II), Co(II), Ni(II), Zn(II), Cd(II), and Hg(II) complexes with a Schiff base ligand, 2-((2-hydroxy-6-methylquinolin-3-yl)methyleneamino)-5-iodobenzoic acid. The complexes were synthesized by reacting the ligand with the corresponding metal chlorides in ethanol, yielding mono- and binuclear species. Structural elucidation was carried out using IR, ¹H NMR, ESR, UV-Vis, X-ray powder diffraction, CHN analysis, conductivity, and magnetic susceptibility measurements. Antimicrobial screening revealed that the free ligand showed low activity, whereas its metal complexes exhibited moderate to good antimicrobial activity.

Keywords: methyl quinoline; 2-amino-5-iodo-bezoic acid; Schiff base and metal complexes; antimicrobial effect.

© 2025 by the authors. This article is an open-access article distributed under the terms and conditions of the Creative Commons Attribution (CC BY) license (<https://creativecommons.org/licenses/by/4.0/>), which permits unrestricted use, distribution, and reproduction in any medium, provided the original work is properly cited. The authors retain copyright of their work, and no permission is required from the authors or the publisher to reuse or distribute this article, as long as proper attribution is given to the original source.

1. Introduction

Schiff bases and their metal complexes have attracted considerable attention due to their diverse applications in biological, clinical, analytical, and pharmacological fields [1,2]. The synthesis of transition metal complexes containing Schiff bases is of particular interest owing to their catalytic potential and significant biological activities. In recent years, metal complexes with ligands containing donor atoms such as nitrogen, oxygen, and sulfur have garnered attention for their remarkable antimicrobial and anticancer properties. Among these, thiazole-based compounds have been extensively studied due to their notable antifungal, antibacterial, and anticancer activities. Thiazole rings are key structural components in vitamin B and the coenzyme thiamine pyrophosphate (carboxylase), playing crucial roles in both structure and function. Schiff bases, formed via the condensation of aromatic or heteroaromatic primary amines with aldehydes or ketones, are classified as imines or azomethines. These compounds represent an important class in medicinal chemistry and pharmaceutical research, exhibiting a wide range of biological activities including antibacterial, antifungal, and antitumor effects [3–

6]. The imine ($-C=N-$) group is often critical to their biological function. With rising mortality due to antibiotic-resistant infections, the search for new antimicrobial agents is urgent [7]. Schiff bases have emerged as promising scaffolds in the development of such agents [8,9]. Particularly, Schiff bases containing dichloro or bromophenyl moieties have shown enhanced biological relevance [6]. The incorporation of halogen atoms increases the lipophilicity of the molecule, thereby improving membrane permeability and enhancing hydrophobic interactions with specific enzyme or receptor binding sites [10]. Among these, salicylidene-based Schiff bases (derived from 2-hydroxybenzaldehyde) have been reported as promising antimicrobial candidates [6,11,12].

A particularly important class of Schiff bases is derived from aromatic aldehydes, as these compounds form stable complexes with various metal ions and are widely utilized as heterogeneous catalysts [12–14]. The azomethine ($-C=N$) linkage present in Schiff bases is a key structural feature responsible for a range of biological activities, including antibacterial, antifungal, and antitumor properties [15–18]. The biological efficacy of these compounds can be further tuned by selecting suitable amines or incorporating specific substituents, particularly functional groups like $-OH$ or $-SH$ positioned near the azomethine group, which enhance metal binding and biological activity [16, 19–24]. Additionally, Schiff base complexes of metals such as platinum and palladium have shown notable antibacterial, antiviral, anti-inflammatory, and anticancer properties [25]. In light of this, we aimed to enhance the biological potential of 2-hydroxy-3-formylquinoline derivatives by synthesizing Schiff bases through their condensation with 3-amino-5-iodo benzoic acid (Scheme 1). These Schiff bases were subsequently used to prepare metal complexes with Zn(II), Cd(II), Hg(II), Ni(II), and Cu(II) (Scheme 2).

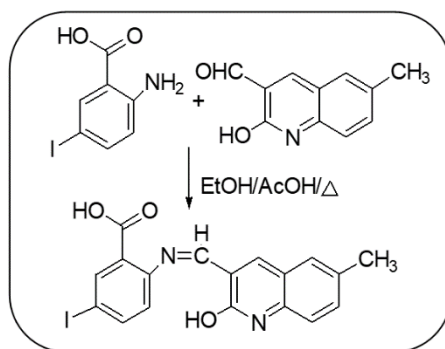
In this study, we report the rational design, synthesis, and antimicrobial evaluation of Schiff base metal complexes formed from 3-amino-5-iodo benzoic acid and 2-hydroxy-3-formylquinoline, with the goal of exploring their potential as bioactive agents.

2. Materials and Methods

All the chemicals used were of analytical grade. 3-amino-5-iodo benzoic acid and 2-hydroxy-3-formyl quinoline were prepared by known methods.

2.1. Synthesis of Schiff base ligand -2-((2-hydroxy-6-methylquinolin-3-yl)methyleneamino)-5-iodobenzoic acid.

An equimolar mixture of 2-amino-5-iodobenzoic acid and 2-hydroxy-3-formylquinoline was dissolved in ethanol and placed in a 100 mL round-bottom flask.

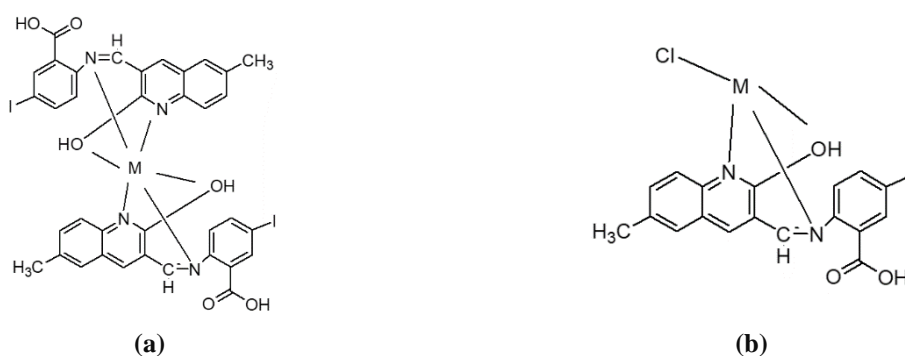


Scheme 1. Schematic route for the synthesis of the ligand.

A few drops of glacial acetic acid were added as a catalyst, and the reaction mixture was refluxed on a water bath for 6–7 hours. Upon completion, the mixture was cooled to room temperature, yielding a yellow crystalline solid. The product was filtered, washed with cold ethanol, and recrystallized from ethanol to afford pure Schiff base. The yield was approximately 85%.

2.2. Preparation of metal complexes.

The hot methanolic solution of the ligand (L) (0.1mg) was agitated for 5 min at 60°C. A hot methanolic solution containing various metal chlorides (Cu(II), Cd(II), and Hg(II) (0.03 mg, 0.025 mg, and 0.026 mg) was added to the reaction mixture, which was then refluxed for 5-6 hrs. The reaction mixture was cooled, then filtered, washed, and dried. The resulting metal complexes were purified by recrystallization in methanol. The metal (II) complexes were dried in an oven and kept in a desiccator.



Scheme 2. Schematic route for the synthesis of metal complex (a) Monomolecular complex of M =Fe(II), Mn(II), Co(II); (b) Bimolecular complex of M=Zn(II), Cd (II), Hg (II), Ni(II), and Cu(II).

2.3. Physical measurements.

The infrared (IR) spectra of the ligand and its metal complexes were recorded in the range of 3800–350 cm⁻¹ using a Perkin Elmer Spectrum One FT-IR spectrometer with KBr pellets. ¹H NMR spectra were obtained on a Bruker AMX-4000 NMR spectrometer using tetramethylsilane (TMS) as an internal standard and DMSO-d₆ as the solvent. Electronic absorption Spectra were recorded in the range of 200–1200 nm using an Elico SL-164 double-beam UV-Visible spectrophotometer in DMF. X-ray powder diffraction patterns were recorded at the Department of Physics, Gulbarga University, Gulbarga. Magnetic susceptibility measurements were performed using the Gouy balance method. Molar conductance measurements were carried out using. An ELICO CM-82 conductivity bridge in DMF at room temperature.

2.4. Antimicrobial screening.

The synthesized compounds were subjected to in vitro biological screening to evaluate their potential as chemotherapeutic agents, based on their structural features. The antimicrobial activity was assessed using the serial dilution method. The synthesized compounds were subjected to in vitro biological screening to evaluate their chemotherapeutic potential, based on their structural characteristics. Antimicrobial activity was assessed using the serial tube dilution method [32] against a panel of seven selected bacterial and fungal strains. Dimethylformamide

(DMF) served as the solvent, and the compounds were tested at concentrations of 200, 100, 50, and 25 ppm. The results are summarized in Table 6.

3. Results and Discussion

3.1. Nature and stoichiometry of ligand.

All the complexes were sparingly soluble in common organic solvents but soluble in DMF, DMSO, and acetonitrile. The analytical data indicate that the complexes agree well with 1:1 metal to ligand stoichiometry for Zn(II), Cd(II), and Hg(II) and 1:2 for Cu(II), Co(II), Ni(II), and Mn(II) complexes, as shown in Table 1. The observed molar conductance values measured in DMF solution fall in the range (14-20 $\Omega^{-1} \text{ cm}^2 \text{ mol}^{-1}$). These observed molar conductance values are well within the expected range for non-electrolytes [20].

Table 1. Analytical, magnetic susceptibility, and molar conductance of the ligand and its metal complexes.

Ligand/ Complex	Mol. Wt.	M.P (°C)	Yield (%)	Found/ calculated (%)					μ_{eff} B.M.	Molar conductance ($\Omega^{-1} \text{ cm}^2 \text{ mol}^{-1}$)
				M	C	H	N	Cl		
[C ₁₈ H ₁₃ IN ₂ O ₃]	432.21	270	75	-	50.02 (49.88)	3.03 (3.08)	6.48 (6.55)	-	-	-
[Cu(C ₃₆ H ₂₈ I ₂ N ₄ O ₈)]	961.98	312	70	6.86 (6.84)	46.70 (46.69)	2.61 (2.56)	6.05 (6.09)	-	1.96	19
[Co(C ₃₆ H ₂₈ I ₂ N ₄ O ₈)]	957.37	320	75	6.40 (6.48)	46.93 (46.68)	2.63 (2.60)	6.08 (6.02)	-	4.74	18
[Ni(C ₃₆ H ₂₈ I ₂ N ₄ O ₈)]	957.13	301	70	6.37 (6.35)	46.94 (46.70)	2.63 (2.60)	6.08 (6.03)	-	2.93	17
[Mn(C ₃₆ H ₂₈ I ₂ N ₄ O ₈)]	953.38	318	75	5.87 (5.92)	46.23 (46.21)	2.80 (2.83)	5.99 (5.94)	-	5.68	14
[Fe(C ₃₆ H ₂₆ I ₂ N ₄ O ₇)Cl]	971.72	340	70	5.75 (5.74)	44.50 (44.44)	2.70 (2.74)	5.77 (5.74)	3.65	5.75	17
[Zn(C ₁₈ H ₁₂ IN ₂ O ₃)Cl]	532.07	348	75	12.29 (12.24)	40.63 (40.60)	2.27 (2.25)	5.27 (5.24)	6.66	Diamagnetic	16
[Cd(C ₁₈ H ₁₄ IN ₂ O ₄)Cl]	597.08	350	80	18.83 (18.80)	36.21 (36.29)	2.36 (2.33)	4.69 (4.63)	5.94	Diamagnetic	14
[Hg(C ₁₈ H ₁₄ IN ₂ O ₄)Cl]	685.26	372	80	29.27 (29.27)	31.55 (31.52)	2.06 (2.05)	4.09 (4.10)	5.17	Diamagnetic	20

3.2. Characterization of Schiff base ligand and its metal complexes.

The Schiff base ligand and its metal complexes were characterized using a combination of spectroscopic and analytical techniques, including ¹H NMR, FT-IR, elemental analysis (CHN), molar conductance, magnetic susceptibility, and thermogravimetric analysis (TGA). The obtained data are in good agreement with the proposed molecular formula of the ligand and its corresponding metal complexes. All synthesized compounds are air-stable, colored solids. They are insoluble in water but exhibit good solubility in polar aprotic solvents such as DMF and DMSO. Molar conductance measurements in DMF at room temperature revealed low values, indicating that all metal complexes behave as non-electrolytes in solution.

3.2.1. Electronic spectra.

The UV–Visible spectra of the free ligand exhibited two characteristic absorption bands at approximately 290 nm, 330 nm, 621 nm, and 914 nm. These bands are attributed to $\pi \rightarrow \pi^*$ and $n \rightarrow \pi^*$ transitions of the azomethine (C=N) chromophore, respectively.

3.2.2. Infrared spectroscopy.

A comparative analysis of the IR spectra of the free ligand and its metal complexes (Table 2) provides evidence for the coordination behavior of the ligand. The free Schiff base shows a prominent absorption band at 1650 cm^{-1} , assigned to the azomethine (C=N) stretching vibration. Additionally, the C=N stretching of the thiazole ring appears in the 1600–1610 cm^{-1} region, and the C–S–C stretching of the thiazole ring is observed between 1405–1408 cm^{-1} . Characteristic vibrations of the substituted thiophene ring are seen at $\sim 3100 \text{ cm}^{-1}$ (C–H), $\sim 1590 \text{ cm}^{-1}$, and $\sim 1405 \text{ cm}^{-1}$, with out-of-plane C–S–C bending observed in the range of 830–850 cm^{-1} . Upon complexation, the azomethine C=N band shifts to lower frequencies by 15–21 cm^{-1} , indicating coordination of the azomethine nitrogen to the metal center. Similarly, the C=N stretching of the thiazole ring also undergoes a downward shift of approximately 15–21 cm^{-1} , suggesting involvement of the thiazole nitrogen in metal coordination. Importantly, the bands associated with the thiophene ring remain largely unchanged, and no M–S vibrational bands are observed in the far-IR region, indicating that the sulfur atom of the thiophene moiety does not participate in coordination. The persistence of C–S–C vibrations and the absence of M–S bands further support this conclusion. New, non-ligand bands in the 405–412 cm^{-1} range observed in the complexes are tentatively assigned to M–N stretching vibrations, supporting metal coordination via nitrogen atoms.

3.2.3. Coordination mode.

Based on these spectroscopic findings, it is evident that the Schiff base ligand acts as a bidentate chelating agent, coordinating to the metal ions via the azomethine and thiazole nitrogen atoms.

Table 2. IR Spectral data of the ligand and its metal complexes (cm^{-1}).

Ligand/ complex	ν_{OH}	$\nu_{\text{C=O}}$	$\nu_{\text{C=N}}$	$\nu_{\text{C-O}}$	$\nu_{\text{M-O}}$	$\nu_{\text{M-N}}$	$\nu_{\text{M-Cl}}$
[C ₁₈ H ₁₃ IN ₂ O ₃]	3435	1662	1599	1209	-	-	-
[Cu(C ₃₆ H ₂₈ I ₂ N ₄ O ₈)]	-	1670	1563	1234	555	478	-
[Co(C ₃₆ H ₂₈ I ₂ N ₄ O ₈)]	-	1684	1560	1260	566	494	-
[Ni(C ₃₆ H ₂₈ I ₂ N ₄ O ₈)]	-	1698	1574	1263	560	482	-
[Mn(C ₃₆ H ₂₈ I ₂ N ₄ O ₈)]	-	1692	1580	1264	556	469	-
[Fe(C ₃₆ H ₂₆ I ₂ N ₄ O ₇)Cl]	-	1683	1558	1234	557	468	360
[Zn(C ₁₈ H ₁₂ IN ₂ O ₃)Cl]	-	1679	1550	1224	552	498	358
[Cd(C ₁₈ H ₁₄ IN ₂ O ₄)Cl]	-	1689	1560	1268	568	482	376
[Hg(C ₁₈ H ₁₄ IN ₂ O ₄)Cl]	-	1697	1555	1240	570	485	394

3.3. ¹H NMR and electronic spectral studies.

The ¹H NMR spectrum of the free Schiff base ligand reveals key signals that confirm the proposed structure. A singlet at δ 7.25 ppm is attributed to the azomethine (–CH=N–) proton, while a nearby singlet at δ 7.20 ppm corresponds to the C–H proton of the thiazole ring. The aromatic region shows the four protons of the phenyl ring as two doublets in the ranges δ 8.17–8.02 ppm and δ 8.04–7.87 ppm. Notably, ligand L1 displays multiplets in the δ 4.21–5.49 ppm range, possibly due to substitution patterns or conformational differences. The spectrum also exhibits a sharp singlet at δ 12.2 ppm (1H), corresponding to the phenolic –OH of the 2-hydroxyquinoline moiety. This peak disappears upon complexation with Zn(II), indicating deprotonation and subsequent coordination through the phenolic oxygen atom [24,25]. Furthermore, the azomethine proton signal shifts slightly from δ 8.8 ppm in the free ligand to δ 8.6 ppm in the Zn(II) complex, suggesting coordination via the azomethine nitrogen [26]. The aromatic protons from both the quinoline and phenyl rings resonate as a broad

multiplet in the region δ 7.0–8.6 ppm in both the free ligand and the Zn(II) complex, further supporting metal coordination.

3.4. Electronic spectra and magnetic susceptibility.

The electronic spectra and magnetic data offer insight into the geometry and electronic environment of the metal complexes: Co(II) Complex: The diffuse reflectance spectrum displays three bands at 9250, 18120, and 19998 cm^{-1} , corresponding to the transitions ${}^4\text{T}_{1g}(\text{F}) \rightarrow {}^4\text{T}_{2g}(\text{F})$, ${}^4\text{T}_{1g}(\text{F}) \rightarrow {}^4\text{A}_{2g}(\text{F})$, and ${}^4\text{T}_{1g}(\text{F}) \rightarrow {}^4\text{T}_{1g}(\text{P})$, respectively. The observed magnetic moment of 4.48 B.M. is consistent with a high-spin octahedral geometry. Ni(II) Complex: Exhibits absorption bands at 13120, 19204, and 26998 cm^{-1} , assigned to ${}^3\text{A}_{2g} \rightarrow {}^3\text{T}_{2g}(\text{F})$, ${}^3\text{A}_{2g} \rightarrow {}^3\text{T}_{1g}(\text{F})$, and ${}^3\text{A}_{2g} \rightarrow {}^3\text{T}_{1g}(\text{P})$ transitions, respectively. The magnetic moment of 3.2 B.M. further confirms an octahedral environment. Cu(II) Complex: Shows three bands at 15374, 15388, and 19997 cm^{-1} , corresponding to ${}^2\text{B}_{1g} \rightarrow {}^2\text{A}_{1g}$, ${}^2\text{B}_{1g} \rightarrow {}^2\text{B}_{2g}$, and ${}^2\text{B}_{1g} \rightarrow {}^2\text{E}_g$ transitions, indicative of a distorted octahedral geometry. The magnetic moment of 1.70 B.M. is typical for mononuclear Cu(II) complexes. Zn(II) Complex: As expected for a d^{10} configuration, the Zn(II) complex is diamagnetic and shows no d–d transitions Table 3. Its spectral silence, along with IR, elemental, and thermal analysis data, supports the formation of an octahedral complex.

Table 3. Electronic spectral data of ligand field parameters of Cu(II), Co(II), Ni(II), and Mn(II) metal complexes.

Complexes	ν_1 (cm^{-1})	ν_2 (cm^{-1})	ν_3 (cm^{-1})	Dq (cm^{-1})	B^1	β	$\beta\%$	ν_2/ν_1	ν_3/ν_2	LFSE (kcal mol^{-1})
[Cu(C ₃₆ H ₂₈ I ₂ N ₄ O ₈)]	12099 – 16049			1420	-	-	-	-	-	24.70
[Co(C ₃₆ H ₂₈ I ₂ N ₄ O ₈)]	9980	15420	21051	930	828	0.96	15.07	1.54	1.36	14.20
[Ni(C ₃₆ H ₂₈ I ₂ N ₄ O ₈)]	8460	16480	25875	912	837	0.84	19.91	1.94	1.57	30.80
[Mn(C ₃₆ H ₂₈ I ₂ N ₄ O ₈)]	9565	17510	21942	939	861	0.82	23.01	1.83	1.25	14.55
[Fe(C ₃₆ H ₂₆ I ₂ N ₄ O ₇)Cl]	11918	14990	19683	940	881	0.80	22.08	1.25	1.31	18.20

3.5. ESR spectral studies.

The ESR spectrum of the powdered Cu(II) complex was recorded at room temperature using diphenylpicrylhydrazyl (DPPH) as a g-marker. The spectrum displayed a broad, unsplit signal, indicating the absence of hyperfine coupling, which is typically attributed to dipolar interactions between copper centers in the solid state. The complex exhibits axial symmetry, with magnetic parameters $g_{\parallel} = 2.237$ and $g_{\perp} = 2.054$. These values are characteristic of a Cu(II) ion in a distorted octahedral geometry. The g-value ($g_{\text{ois}} = (g_{\parallel} + 2g_{\perp})/3$) further supports this assignment. The exchange interaction parameter G, calculated using Hathway's expression [27] $G = g_{\parallel} - 2.0023g_{\perp} - 2.0023G = \frac{g_{\parallel} - 2.0023}{g_{\perp} - 2.0023}G = g_{\perp} - 2.0023g_{\parallel} - 2.0023$, was found to be 4.338. According to Hathway, a G value greater than 4 suggests negligible exchange interaction between adjacent copper centers, while a value below 4 indicates significant interaction. Thus, the observed G value confirms the mononuclear nature of the Cu(II) complex in the solid state.

Table 4. ESR spectral data of the Cu(II) complex.

Complex	g_{\parallel}	g_{\perp}	g_{av}	g_{iso}	G
[Cu(C ₃₆ H ₂₈ I ₂ N ₄ O ₈)]	2.235	2.054	2.144	2.189	4.338

3.6. Thermogravimetric analysis (TGA).

The thermal stability and decomposition behavior of the synthesized metal complexes were examined using thermogravimetric analysis. All the complexes exhibited good thermal stability up to 60–70°C, indicating the absence of loosely bound solvent molecules. The decomposition profiles occurred in three distinct stages: The first stage (up to ~140°C) corresponds to the loss of coordinated water molecules—one molecule in the Co(II), Ni(II), and Cu(II) complexes, and two molecules in the Zn(II) complex. The second stage (220–240°C) is attributed to the decomposition of organic moieties within the ligand framework. The third stage, observed at higher temperatures, corresponds to complete degradation of the organic matrix, ultimately leading to the formation of stable metal oxide residues. These thermal transitions support the proposed coordination of water molecules and confirm the structural stability of the complexes under moderate heating.

Table 5. X-ray powder diffraction data of Cu(II) complex of the ligand.

2θ	θ	sinθ	Sin ² θ	h ² +k ² +l ² (a)	h ² +k ² +l ² (b)	hkl	d-spacing		Relative intensity (%)	a (Å)
							Cal.	Abs		
5.691	2.845	0.049	0.002	1	1	100	15.517	15.517	5.36	11.46
11.719	5.859	0.102	0.010	3.6	4	200	7.544	7.544	15.69	11.46
14.437	7.218	0.125	0.015	6.6	7	310	6.127	6.127	25.44	11.46
19.766	9.883	0.171	0.029	13.7	14	321	4.487	4.487	100.00	11.46
27.463	13.731	0.237	0.056	4.6	5	210	3.244	3.244	47.89	11.46
32.596	16.299	0.280	0.078	5.9	6	211	2.744	2.744	9.481	11.46
36.426	18.213	0.312	0.097	4.4	4	200	2.464	2.464	8.245	11.46
39.150	19.575	0.335	0.112	5.7	6	211	6.078	6.078	5.36	11.46
58.290	29.140	0.486	0.236	9.2	9	221	1.580	1.580	8.82	11.46

3.7. Magnetic susceptibility studies and electronic spectra of the complexes.

3.7.1. Magnetic and electronic spectral studies of Cu(II) complex.

The Cu(II) complexes exhibit temperature-independent magnetic moments in the range of 1.74–2.20 B.M., which are consistent with the spin-only value of 1.72 B.M. for a single unpaired electron. The observed value of 1.90 B.M. for the present Cu(II) complex falls within the expected range and suggests the presence of mononuclear species with no significant spin-spin interactions. The slight deviation from the spin-only value is commonly attributed to spin-orbit coupling. These observations indicate that the Cu(II) complexes possess a distorted octahedral geometry, supported by both magnetic and spectral data. The absence of magnetic exchange coupling suggests isolated metal centers, while the observed magnetic moment and geometry distortion are typical for d⁹ systems exhibiting Jahn–Teller distortion. The electronic spectra of the Cu(II) complexes exhibit broad, low-intensity shoulder bands in the range of 12099–16580 cm⁻¹, characteristic of d–d transitions in an octahedral Cu(II) (d⁹) ion undergoing tetragonal distortion. In such distorted octahedral environments, the expected transitions ²B_{1g} → ²B_{2g}, ²B_{1g} → ²E_g, and ²B_{1g} → ²A_{1g}—are often unresolved and appear as a single broad asymmetric band, commonly observed on the lower energy side of the spectrum [23]. The band maxima for the present Cu(II) complexes were recorded at 12099 cm⁻¹, 12745 cm⁻¹, and 16049 cm⁻¹, all consistent with six-coordinate octahedral structures.

Additionally, a high-intensity band observed around 15640 cm⁻¹ is attributed to ligand-to-metal charge transfer (LMCT) transitions [24]. The charge transfer bands in the region 25400–31000 cm⁻¹ further support the involvement of ligand orbitals in metal coordination and confirm the distorted octahedral geometry around the Cu(II) center. The broadness and

asymmetry of these bands provide additional evidence for dynamic Jahn–Teller distortion, a common feature in Cu(II) octahedral complexes.

3.7.2. Cobalt(II) complex.

In octahedral Co(II) complexes, the ground state term is ${}^4T_{1g}(F)$, and significant orbital contributions typically result in magnetic moment values ranging between 4.6–5.18 B.M. for octahedral geometries, and 4.11–4.78 B.M. for tetrahedral geometries. In the present investigation, the Co(II) complex exhibited a magnetic moment of 4.68 B.M. [25], suggesting an octahedral geometry with partial quenching of orbital contribution. The electronic spectrum of the Co(II) complex shows three distinct absorption bands at: 9980 cm^{-1} (${}^4T_{1g}(F) \rightarrow {}^4T_{2g}(F)$, ν_1), 15420 cm^{-1} (${}^4T_{1g}(F) \rightarrow {}^4A_{2g}(F)$, ν_2), 21051 cm^{-1} (${}^4T_{1g}(F) \rightarrow {}^4T_{1g}(P)$, ν_3), along with a charge transfer band at 25650 cm^{-1} . These spectral features are consistent with reported literature values [26,27] and confirm an octahedral coordination environment around the Co(II) ion.

3.7.3. Nickel(II) complex.

The Ni(II) complex exhibited a magnetic moment of 4.70 B.M., which is within the expected range for octahedral Ni(II) complexes [26]. In an octahedral field, the ground state term is ${}^3A_{2g}(F)$, and three spin-allowed transitions are typically observed. The electronic spectrum revealed three absorption bands at: 8460 cm^{-1} (${}^3A_{2g}(F) \rightarrow {}^3T_{2g}(F)$, ν_1), 16480 cm^{-1} (${}^3A_{2g}(F) \rightarrow {}^3T_{1g}(F)$, ν_2), 25875 cm^{-1} (${}^3A_{2g}(F) \rightarrow {}^3T_{1g}(P)$, ν_3). These transitions fall within the expected ranges and indicate considerable covalent character, supporting an octahedral geometry for the Ni(II) complex [28].

3.7.4. Manganese(II) complex.

The Mn(II) complex shows a magnetic moment of 5.50 B.M., which is characteristic of a high-spin d^5 configuration and consistent with the presence of five unpaired electrons. The electronic spectrum displays three bands at: 9565 cm^{-1} (${}^6A_{1g} \rightarrow {}^4T_{1g}({}^4G)$, ν_1), 17510 cm^{-1} (${}^6A_{1g} \rightarrow {}^4E_g({}^4D)$, ν_2), 21942 cm^{-1} (${}^6A_{1g} \rightarrow {}^4T_{1g}({}^4D)$, ν_3). These transitions suggest considerable covalent bonding and are in line with an octahedral geometry around the Mn(II) ion [30].

3.7.5. Iron(III) complex.

The Fe(III) complex exhibited a magnetic moment of 5.72 B.M., typical for high-spin Fe(III) (d^5) complexes with five unpaired electrons in an octahedral field. Its electronic spectrum shows three absorption bands at: 11918 cm^{-1} (${}^6A_{1g} \rightarrow {}^4T_{1g}({}^4G)$, ν_1), 14990 cm^{-1} (${}^6A_{1g} \rightarrow {}^4E_g({}^4D)$, ν_2), 19683 cm^{-1} (${}^6A_{1g} \rightarrow {}^4T_{1g}({}^4D)$, ν_3). These transitions, along with the observed covalent character, strongly support an octahedral geometry for the Fe(III) complex [29].

Table 6. Antimicrobial activity of synthesized compounds (MIC).

Compound	Antibacterial activity		Antifungal activity	
	<i>E. coli</i>	<i>S. typhi</i>	<i>C. albicans</i>	<i>A. niger</i>
[C ₁₈ H ₁₃ IN ₂ O ₃]	200	200	50	50
[Cu(C ₃₆ H ₂₈ I ₂ N ₄ O ₈)H ₂ O/2]	50	50	100	100
[Co(C ₃₆ H ₂₈ I ₂ N ₄ O ₈)H ₂ O/2]	100	100	100	100
[Ni(C ₃₆ H ₂₈ I ₂ N ₄ O ₈)H ₂ O/2]	200	100	100	200
[Mn(C ₃₆ H ₂₈ I ₂ N ₄ O ₈)H ₂ O/2]	200	100	200	200
[Fe(C ₃₆ H ₂₆ I ₂ N ₄ O ₇)ClH ₂ O/2]	100	200	200	200
Gentamycin (Std)	25	25	---	---
Fluconazole (Std)	---	---	25	25

3.8. Antimicrobial activity.

The antimicrobial screening of the Schiff base ligand and its metal complexes revealed diverse antibacterial and antifungal profiles. The free ligand displayed notable antifungal activity, confirming its intrinsic bioactivity. Among all the synthesized metal complexes, the Cu(II) complex exhibited the most potent and broad-spectrum antimicrobial activity, especially against fungal strains. The Co(II), Ni(II), Zn(II), Cd(II), and Hg(II) complexes showed moderate antibacterial and antifungal activity compared to the standard reference drugs. The enhanced activity of the metal complexes over the free ligand is attributed to metal coordination, which increases lipophilicity, improves membrane permeability, and promotes stronger interactions with microbial targets. These findings establish that complexation significantly enhances the biological efficacy of the Schiff base, with the Cu(II) complex emerging as a promising lead compound for future therapeutic development.

4. Conclusion

A new series of coordination complexes of Cu(II), Co(II), Ni(II), Zn(II), Cd(II), and Hg(II) with the Schiff base ligand 2-((2-hydroxy-6-methylquinolin-3-yl)methyleneamino)-5-iodobenzoic acid have been successfully synthesized and comprehensively characterized using elemental analysis (CHN), molar conductivity, magnetic susceptibility, IR, ¹H NMR, ESR, UV-Vis, and X-ray powder diffraction techniques. Spectroscopic and magnetic data confirm that the Cu(II), Co(II), Ni(II), and Mn(II) complexes adopt octahedral geometries, while the Zn(II), Cd(II), and Hg(II) complexes exhibit tetrahedral geometries. These results highlight the structural flexibility and coordination adaptability of the Schiff base ligand, enabling the formation of thermally stable, geometrically diverse metal complexes depending on the nature of the central metal ion.

Author Contributions

Data curation, P.C.; writing—original draft preparation, P.C.; writing—review and editing, P.C.; supervision, P.C.; project administration, P.C.; investigation, P.C.; methodology, N.M.M.; funding acquisition, P.C.H.; conceptualization, P.C.H.; validation, P.N.P.; formal analysis, P.N.P.; resources, V.J.B.; visualization, T.A. All authors have read and agreed to the published version of the manuscript.

Institutional Review Board Statement

Not applicable.

Informed Consent Statement

Not applicable.

Data Availability Statement

Data supporting the findings of this study are available upon reasonable request from the corresponding author.

Funding

This research received no external funding.

Acknowledgments

The authors are thankful to the Principal of Sahyadri Science College, Shivamogga, for providing an experimental facility, and to the chairman, Dept. of Biotechnology, Gulbarga University, Gulbarga, for carrying out experimental work and biological evaluation. SAIF Chandigarh for spectra data.

Conflicts of Interest

The authors declare no conflict of interest.

References

1. Poojari, S.; Naik, P.; Krishnamurthy, G. Synthesis of macrocycles containing 1,3,4-oxadiazole and pyridine moieties. *Tetrahedron Letters* **2014**, *55*, 305-309, <https://doi.org/10.1016/j.tetlet.2013.08.099s>.
2. Naik, S.; Naik, P.P.; Krishnamurthy, G.; Venugopal, N.; Naik, N.; Naik, T.R. Synthesis, Characterization, DFT Studies and Biological Activity of Ru(III), La(III) and Ce(III) Triphenylphosphine Complexes Containing 2-Aminothiazole and 2-Aminotriazole. *J. Inorg. Organomet. Polym. Mater.* **2020**, *30*, 3332, <https://doi.org/10.1007/s10904-020-01492-y>.
3. Pachaiappan, R.; Rajendran, S.; Show, P.L.; Manavalan, K.; Naushad, M. Metal/metal oxide nanocomposites for bactericidal effect: A review. *Chemosphere* **2021**, *272*, 128607, <https://doi.org/10.1016/j.chemosphere.2020.128607>.
4. Mohamed, G.G.; Omar, M.M.; Ahmed, Y.M.; Metal complexes of tridentate Schiff base: Synthesis, characterization, biological activity and molecular docking studies with COVID-19 protein receptor. *J. Inorg. Gen. Chem.* **2021**, *647*, 2201-2218, <https://doi.org/10.1002/zaac.202100245>.
5. Sumra, S.H.; Mushtaq, F.; Ahmad, F.; Hussain, R.; Zafar, W.; Imran, M.; Zafar, M.N. Coordination behavior, structural, statistical and theoretical investigation of biologically active metal-based isatin compounds. *Chem. Pap.* **2022**, *76*, 3705-3727, <https://doi.org/10.1007/s11696-022-02123-1>.
6. Redrado, M.; Xiao, Z.; Upitak, K.; Doan, B.T.; Thomas, C.M.; Gasser, G. Applications of Biodegradable Polymers in the Encapsulation of Anticancer Metal Complexes. *Advanced Functional Materials* **2024**, *34*, 2401950, <https://doi.org/10.1002/adfm.202401950>.
7. Cosgrove, S.E. The relationship between antimicrobial resistance and patient outcomes: mortality, length of hospital stay, and health care costs. *Clin. Infect. Dis.* **2006**, *42*, S82-S89, <https://doi.org/10.1086/499406>.
8. Nechipadappu, S.K.; Ramachandran, J.; Shivalingegowda, N.; Lokanath, N.K.; Trivedi, D.R. Synthesis of cocrystals/salts of flucytosine: Structure and stability. *New Journal of Chemistry* **2018**, *42*, 5433-5446, <https://doi.org/10.1039/C7NJ04400C>.
9. Naik, S.; Paramashwara Naik, P.; Krishnamurthy, G. Synthesis, Characterization, DFT, DNA binding/cleavage studies of Schiff base metal (II) complexes. *Res. J. Chem. Environ.* **2020**, *24*, 93-103.
10. Karthikeyan, M.S.; Prasad, D.J.; Poojary, B.; Bhat, K.S.; Holla, B.S.; Kumarib, N.S. Synthesis and Biological Activity of Schiff and Mannich Bases Bearing 2,4-Dichloro-5-Fluorophenyl Moiety. *Bioorg. Med. Chem.* **2006**, *14*, 7482, <http://dx.doi.org/10.1016/j.bmc.2006.07.015>.
11. De, Souza A.O.; Galetti, F.C.S.; Silva, C.L.; Bicalho, B.; Parma, M.M.; Fonseca, S.F.; Marsaioli, A.J.; Trindade, A.C.L.B.; Rossimíriam, P.; Gil, F.; Bezerra, F.S.; Andrade-Neto, M.; de Oliveira, M.C.F. Antimycobacterial and Cytotoxicity Activity of Synthetic and Natural Compounds. *Quim Nova.* **2007**, *30*, 1563, <https://doi.org/10.1590/S0100-40422007000700012>.
12. Abdelwahab, H.; Hassan, S.; Yacout, G.; Mostafa, M.; El Sadek, M. Synthesis and biological evaluation of new imine- and amino-chitosan derivatives. *Polymers* **2015**, *7*, 2690-2700, <http://dx.doi.org/10.3390/polym7121532>.
13. Melkeri, S.P.; Naik, P.P.; Satyanarayan, N.D.; Pushpavathi, I.; Krishnamurthy, G.; Chavan, P.W. Synthesis and Characterization of Biopotent Transition Metal Complexes of Schiff Base 2-[(1)-1-[2-(1,3-

- Benzothiazol-2-yl)hydrazinylidene]ethyl}-6,10b-dihydro-3H-benzo[f]chromen-3-one and their Biological Evaluation. *Asian Journal of Chemistry* **2024**, *36*, 844-850, <https://doi.org/10.14233/ajchem.2024.31148>
14. Baran, T. A new chitosan Schiff base supported Pd(II) complex for microwave-assisted synthesis of biaryl compounds. *J. Mol. Struct.* **2017**, *1141*, 535, <https://doi.org/10.1016/j.molstruc.2017.03.122>.
 15. Renata, P.; Małgorzata, W. S.; Sabina, J.; Tomasz, K.; Marcelina, K.; Anna, H. Latest developments in metal complexes as anticancer agents. *Coordination Chemistry Reviews.* **2022**, *452*, 214307. <https://doi.org/10.1016/j.ccr.2021.214307>.
 16. Elshaarawy, R.F.M.; Refaee, A.A.; El-Sawi, E.A. Pharmacological performance of novel poly-(ionic liquid)-grafted chitosan-*N*-salicylidene schiff bases and their complexes. *Carbohydr. Polym.* **2016**, *146*, 376, <https://doi.org/10.1016/j.carbpol.2016.03.017>.
 17. Raman, N.; Selvan, A.; Sudharsan, S. Metallation of ethylenediamine based schiff base with biologically active Cu(II), Ni(II) and Zn(II) ions: Synthesis, spectroscopic characterization, electrochemical behaviour, DNA binding, photonuclease activity and in vitro antimicrobial efficacy. *Spectrochim. Acta A.* **2011**, *79*, 873-883, <https://doi.org/10.1016/j.saa.2011.03.017>.
 18. Salama, H.E.; Saad, G.R.; Sabaa, M.W. Synthesis, characterization and biological activity of Schiff bases based on chitosan and arylpyrazole moiety. *Int. J. Biol. Macromol.* **2015**, *79*, 996-1003, <https://doi.org/10.1016/j.ijbiomac.2015.06.009>.
 19. Wardha, Z.; Muhammad, A.; Sajjad, H. Sumrra. A review on the antimicrobial assessment of triazole-azomethine functionalized frameworks incorporating transition metals. *Journal of Molecular Structure* **2023**, *1288*, 135744, <https://doi.org/10.1016/j.molstruc.2023.135744>.
 20. Araújo, E.L.; Barbosa, H.F.G.; Dockal, E.R.; Cavalheiro, É.T.G. Synthesis, characterization and biological activity of Cu(II), Ni(II) and Zn(II) complexes of biopolymeric Schiff bases of salicylaldehydes and chitosan. *Int. J. Biol. Macromol.* **2017**, *95*, 168-176, <https://doi.org/10.1016/j.ijbiomac.2016.10.109>.
 21. Abrar, Ul, H.; Sajjad, H.S.; Muhammad, I.; Zahid Hussain, C. New 3d multifunctional metal chelates of sulfonamide: Spectral, vibrational, molecular modeling, DFT, medicinal and *in silico* studies. *Journal of Molecular Structure.* **2022**, *1254*, 132305, <https://doi.org/10.1016/j.molstruc.2021.132305>.
 22. Janjua, U.; Pervaiz M.; Ali F.; Saleem A.; Ashraf A.; Younas U.; M. Iqbal.; Schiff base derived Mn(II) and Cd(II) novel complexes for catalytic and antioxidant applications. *Inorg. Chem. Commun.* **2023**, *157*, 111233, <https://doi.org/10.1016/j.inoche.2023.111233>.
 23. Sadaf, N.; Sajjad, H.S.; Zahid, H.C.; Ghulam, M.; Muhammad, I. Synthesis, characterization, molecular docking and network pharmacology of bioactive metallic sulfonamide-isatin ligands against promising drug targets. *Journal of Molecular Structure* **2023**, *1277*, 134780, <https://doi.org/10.1016/j.molstruc.2022.134780>.
 24. Dhananjay, G. Palke. Synthesis, Physicochemical and Biological Studies of Transition Metal Complexes of DHA Schiff Bases of Aromatic Amine. *Journal of Applied Oragnometalic Chemistry* **2022**, *2*, 81, <https://doi.org/10.22034/jaoc.2022.349187.1055>.
 25. Gracelin Retnam, C.T.; Viola Rose, S.; Sindhu Kumari, B. Synthesis, characterization, biological activity and molecular docking study of transition metal complexes from heterocyclic ligand system. *Journal of Molecular Structure* **2023**, *1282*, 135162, <https://doi.org/10.1016/j.molstruc.2023.135162>.
 26. Vasantakumarnaik, N.K.; Krishnamurthy, G.; Malathesh, Pari.; Ranjitha, N.; Anilkumara, H.A.; Akarsh, G.Y.; Manjunatha, M.N. Synthesis, characterization of 4-[(E)-{2-hydroxy-3-[(Z)-1,3-thiazol-2-yl)diazenyl]naphthalen-1-yl)methylidene] amino}benzoic acid and its transition metal complexes; biopharmaceutical activities and electrochemical detection of ciplactin. *Journal of Molecular Structure* **2023**, *1294*, 136405, <https://doi.org/10.1016/j.molstruc.2023.136405>.
 27. Ghanghas, P.; Choudhary, A.; Kumar, D.; Poonia, K. Coordination metal complexes with Schiff bases: Useful pharmacophores with comprehensive biological applications. *Inorg. Chem. Commun.* **2021**, *130*, 108710, <https://doi.org/10.1016/j.inoche.2021.108710>.
 28. Aroua, L.M.; Alhag, S.K.; Al-Shuraym, L.A.; Messaoudi, S.; Mahyoub, J.A.; Alfaihi, M.Y.; Al-Otaibi, W.M. Synthesis and characterization of different complexes derived from Schiff base and evaluation as a potential anticancer, antimicrobial, and insecticide agent. *Saudi Journal of Biological Sciences* **2023**, *30*, 103598, <https://doi.org/10.1016/j.sjbs.2023.103598>.
 29. Ngoepe, M.P.; Clayton, H.S. Metal Complexes as DNA Synthesis and/or Repair Inhibitors: Anticancer and Antimicrobial Agents. *Pharm. Fronts.* **2021**, *3*, e164–e182, <https://doi.org/10.1055/s-0041-1741035>.

30. Singh, P.; Yadav, P.; Sodhi, K.K.; Tomer, A.; Mehta, S.B. Advancement in the synthesis of metal complexes with special emphasis on Schiff base ligands and their important biological aspects. *Results in Chemistry* **2024**, *7*, 101222, <https://doi.org/10.1016/j.rechem.2023.101222>.
31. Kargar, H.; Fallah-Mehrjardi, M.; Behjatmanesh-Ardakani, R.; Rudbari, H.A.; Ardakani, A.A.; Sedighi-Khavidak, S.; Munawarf, K.S.; Ashfaq, M.; Tahir, M.N. Synthesis, spectral characterization, crystal structures, biological activities, theoretical calculations and substitution effect of salicylidene ligand on the nature of mono and dinuclear Zn(II) Schiff base complexes. *Polyhedron* **2022**, *213*, 115636, <https://doi.org/10.1016/j.poly.2021.115636>.
32. Chavan, P.; Hanamshetty, P.C.; Biradar, B.; Nagabhushan, M. Design and Synthesis of Novel 1, 4-Dihydropyridine Derivatives as Antioxidant and Antimicrobial Agents. *Russian Journal of Organic Chemistry* **2024**, *60*, 912-917, <https://doi.org/10.1134/S1070428024050130>.

Publisher's Note & Disclaimer

The statements, opinions, and data presented in this publication are solely those of the individual author(s) and contributor(s) and do not necessarily reflect the views of the publisher and/or the editor(s). The publisher and/or the editor(s) disclaim any responsibility for the accuracy, completeness, or reliability of the content. Neither the publisher nor the editor(s) assume any legal liability for any errors, omissions, or consequences arising from the use of the information presented in this publication. Furthermore, the publisher and/or the editor(s) disclaim any liability for any injury, damage, or loss to persons or property that may result from the use of any ideas, methods, instructions, or products mentioned in the content. Readers are encouraged to independently verify any information before relying on it, and the publisher assumes no responsibility for any consequences arising from the use of materials contained in this publication.